DOI 10.1007/s11062-022-09922-y
Neurophysiology, Vol. 53, No. 2, March, 2021

Binary Particle Swarm Optimization-Based Feature Selection for Predicting the Class of the Knee Angle from EMG Signals in Lower Limb Movements

I. S. Dhindsa,[1] R. Gupta,[2] and R. Agarwal[3]

Received November 26, 2020

The performance of a binary particle swarm optimization-based feature selection (BPSOFS) for predicting the class of the knee angle (KA) from myoelectric signals in lower limb movements was examined. Surface EMG (sEMG) signals were recorded from the *vastus lateralis* and *biceps femoris* muscles while performing a task of standing up from and sitting down on the chair. The knee angle was measured using a goniometer and quantized into five levels/classes. The sEMG signals were segmented using overlapped windowing. Twenty features per muscle were extracted and fed to a support vector machine (SVM) classifier. Grid selection was done to set the parameters of the classifier. In our study, the KA was first divided into five levels/classes, and the KA class was predicted from the features of sEMG signals using the SVM classifier. Subsequently, BPSOFS was implemented, and the classification accuracy was measured using a reduced feature set. The performance of three different initialization techniques, namely small, large, and mixed initializations, were compared. A paired *t* test was applied to compare the performance of the SVM classifier with BPSOFS and with the SVM classifier using all the features. The results indicated that BPSOFS achieves a classification accuracy of 90.92% utilizing only 30% of the total features ($P > 0.05$).

Keywords: lower limb movements, knee joint angle, surface electromyography, feature selection, particle swarm optimization, support vector machine.

INTRODUCTION

Feature selection involves finding a subset of the x features from a set of the X features, $x < X$, without significantly decreasing the classification/prediction accuracy. Feature selection offers many advantages, such as a reduced training time, a smaller storage requirement, and simple data visualization [1]. Such selection is a rather complex task. For the same data, many different feature subsets achieving the same prediction accuracy may be found [2].

There are complex interactions among features. An individually relevant feature can become redundant when working together with other features. The selection of such a feature results in redundancy, which degrades the classifier performance. A feature that is weakly relevant can significantly improve the classification accuracy (CA) if it is complementary to some other features. Therefore, the removal of such a feature may result in a poorer feature subset. Although many feature selection algorithms have been proposed, most of them suffer from either high computational cost due to a large search space or the problems of stagnation in the local optima. Therefore, an efficient global search technique is needed to address feature selection tasks.

Particle swarm optimization (PSO) is a simple optimization technique inspired from the social behavior of birds flocking and fish schooling. Birds and fish adjust their physical movements to avoid predators, seek food and/or mates, optimize

[1] Electronics and Communication Engineering Department, Government Polytechnic, Ambala City, India.
[2] Electrical Engineering Department, Indian Institute of Technology Delhi, New Delhi, India.
[3] Electrical and Instrumentation Engineering Department, TIET, Patiala, Punjab, India.
Correspondence should be addressed to R. Gupta (rohit.udai@yahoo.co.in).

environmental parameters (e.g., temperature), etc. The most important advantage of PSO is its simplicity. It can be materialized using very few lines of code, requires only elementary mathematical operations, requires less memory, and is characterized by a high speed [3].

Several myoelectrically controlled techniques for managing the upper limb prosthetic/orthotic devices were proposed within the last two decades. Some of those were based on time domain features (TDFs) [4–7], some others utilized frequency domain features (FDFs) [8], and some used time-frequency analysis, such as short-time Fourier transform (STFT) [9] or wavelets [10, 11]. In the case of the lower limb, the research has been limited to predicting the locomotion modes, such as level-ground walking and ascending/descending via ramps and stairs [12–16]. Prediction of the knee angle (KA) plays a vital role in the performance of the prosthetic, estimating the intended posture. Prediction of the KA from EMG signals using pattern recognition was proposed [17–19]. In our present study, feature selection using a binary particle swarm optimization (BPSO) technique has been studied for predicting the KA from surface electromyographic (sEMG) signals recorded from the *vastus lateralis* (VL) and *biceps femoris* (BF) muscles of the lower limb.

The rest of the paper is arranged as follows. The PSO technique is briefly explained, the methodology adopted in the present study is discussed, and, finally, the results are presented.

Particle swarm optimization (PSO) is a population-based search algorithm that was proposed by Kennedy and Eberhart in 1995 [3]. This algorithm is based on the principle that each solution can be represented as a particle in the swarm. The position of the i^{th} particle within the search space is represented by a vector $x_i = \left(x_{i,1}, x_{i,2}, \cdots, x_{i,D}\right)$, where D is the dimensionality of the search space. To search for an optimal solution, each particle moves within the search space with a velocity v; the velocity of the i^{th} particle is represented by the vector $v_i = \left(v_{i,1}, v_{i,2}, \cdots, v_{i,D}\right)$. Each particle updates its velocity on the basis of its past experience and the past experience of the swarm. The velocity of the particles is updated in consideration of its previous best position P_{best} and the swarm's previous best position G_{best}. The velocity of the particle is updated according to Eq.1

$$v_{i,d}\left(t+1\right) = w \cdot v_{i,d}\left(t\right) + C_1 r_1 \left(P_{i,d} - x_{i,d}\left(t\right)\right) + \\ + C_2 r_2 \left(P_{g,d} - x_{i,d}\left(t\right)\right), \quad (1)$$

where r_1 and r_2 are random functions having a value between 0 and 1, w is the inertial weight, $P_{g,d}$ is the G_{best} position in the swarm, $P_{i,d}$ is the P_{best} position of the i^{th} particle, C_1 is the personal learning factor, and C_2 is the social learning factor. The velocity $v_{i,d}$ is limited within the predefined range $[v_{min}, v_{max}]$. The value of v_{max} regulates the resolution of the search space between the present and the target positions [20]. The value of v_{max} must be kept within 10–20% of the dynamic range of the particle's position [21]. The position of the i^{th} particle is updated according to Eq. 2.

$$x_{i,d}\left(t+1\right) = x_{i,d} + v_{i,d}\left(t+1\right), \quad (2)$$

Kennedy and Eberhart [22] proposed a discrete version of PSO and named it binary PSO (BPSO). In this technique, each particle moves within a state space restricted to 0 and 1 on each dimension [22]. The velocity of the i^{th} particle $v_{i,d}$ is obtained similar to the continuous PSO, as in Eq. 1, with a modification that $x_{i,d}$, $P_{i,d}$, and $P_{g,d}$ are integers either 0 or 1. The particle position is obtained using Eq.3:

$$x_{i,d}\left(t+1\right) = \begin{cases} 1 & r_3(\ ) < F_1\left(v_{i,d}\left(t\right)\right) \\ 0 & Otherwise \end{cases} \quad (3)$$

where $F_1\left(x\right)$ is a sigmoid function evaluated according to Eq.4 and $r_3()$ is a random number within the range [0.0,1.0].

METHODS

Twelve male subjects (S_1–S_{12}) with a mean age of 31.08±3.15 years, body mass 81.42±9.5 kg, and height 1.72±0.08 m gave informed consent to take part in this study. Subjects were initially made to sit on a chair and then were asked to perform ten sets of stand-ups from chair and sit-downs on the chair at a reasonable rate. Five trials were performed daily with a rest period of 15 min between successive trials. This routine was carried out for 5 days for each subject. Figure 1 shows the block diagram of the KA prediction system.

Data collection. The sEMG signals from the VL and BF of the lower limb were collected using the Nexus-10 biofeedback system that provided sampling at 2048 samples/sec. The justification

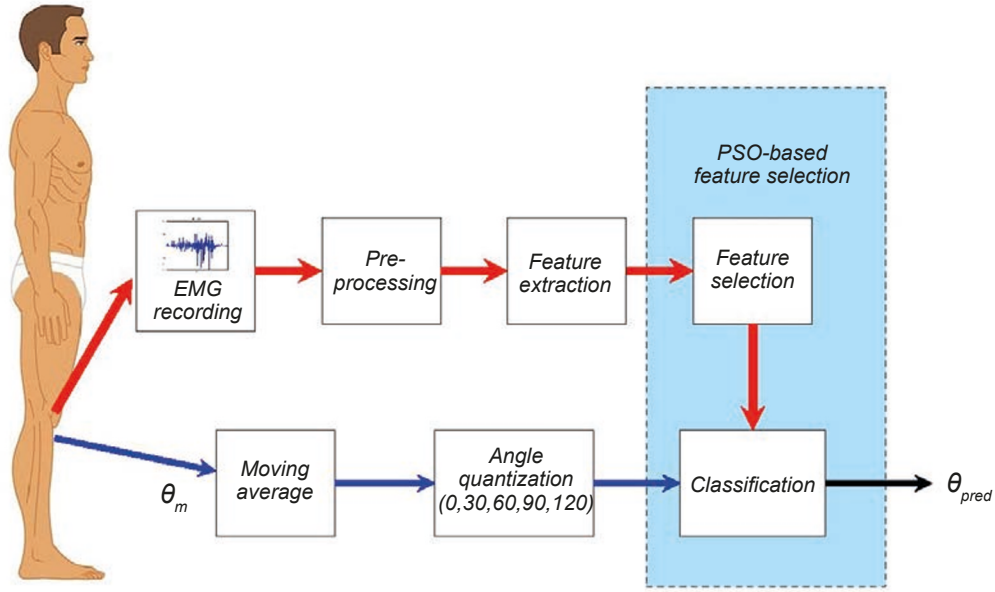

F i g. 1. Block diagram of the system. PSO, particle swarm optimization.

for selecting these two muscles was explained earlier [23]. Bipolar Ag/AgCl electrodes with a 20-mm interelectrode distance were used to obtain the sEMG signal. The SENIAM recommendations for the placement of electrodes were followed [24]. The sensor locations for muscles used in the present study are given in Table 1. The KA was measured using a precision potentiometer-based goniometer. The voltage signal at the output of the goniometer was digitized using the NI-6009 data acquisition system and NI LabView 2013 software. The measured KA was low pass-filtered using a 4th order IIR Butterworth filter (F_C = 2 Hz).

Feature extraction. The random nature of the EMG signal makes the instantaneous value of the EMG inappropriate for control purposes [25]. Classification of the patterns using raw myoelectric signals results in a poor classification accuracy, which is unsatisfactory for the prosthetic control purposes [26]. Therefore, sEMG signals were segmented using moving windows for the data analysis, and features were extracted. The current study used an overlapped windowing technique with a window size of 256 msec and a window increment of 128 msec. The justification of the window size was explained in the previous work [14]. Twenty EMG features were evaluated for each muscle. Table 2 gives the details of the features used in the present study. All the features obtained for a window together constitute a feature vector. The feature vector F_W for the W^{th} window is given by Eq.5.

$$F_W = \left[f_{1,1}, \cdots, f_{i,j}, \cdots, f_{2,20} \right], \qquad (5)$$

where i represents the muscle number, and j is the feature number.

An attribute/feature having a greater numerical range has a fair chance of dominating other attributes having lower numerical ranges. To prevent this, the feature vector is normalized using a min–max normalization technique, mathematically given by Eq.6:

$$F_{norm}(i) = \frac{f_i - min_i}{max_i - min_i}, \qquad (6)$$

where max_i is the maximum value, and min_i is the minimum value of the i^{th} feature respectively, and f_i is the value of the i^{th} feature.

T a b l e 1. Sensor Location for sEMG Recording

No	Muscle	Sensor position
1	*Vastus lateralis* (VL)	At 2/3 on the line from the anterior *spina iliaca* superior to the lateral side of the *patella*
2	*Biceps femoris* (BF)	At 50% on the line between the ischial tuberosity and the lateral epicondyle of the *tibia*
3	Reference	On the *tibia* bone

T a b l e 2. sEMG Features Used in the Present Study

No.	Feature Name	Equation
1	Integral EMG (iEMG)	$\sum_{i=1}^{N}\lvert x_i\rvert$
2	EMG average rectified value (ARV)	$\frac{1}{N}\sum_{i=1}^{N}\lvert x_i\rvert$
3	EMG variance (VAR)	$\frac{1}{N-1}\sum_{i=1}^{N}x_i^2$
4	Simple square integral (SSI)	$\sum_{i=1}^{N}x_i^2$
5	Root mean square (RMS)	$\sqrt{\frac{1}{N}\sum_{i=1}^{N}x_i^2}$
6	Waveform length (WL)	$\sum_{i=2}^{N}\lvert x_i - x_{i-1}\rvert$
7	Willison amplitude (WAMP)	$\sum_{i=2}^{N}\left[f\left(\lvert x_i - x_{i-1}\rvert\right)\right]$ where $F(x)=\begin{cases}1 & x > Threshold\\ 0 & Otherwise\end{cases}$
8	Mean frequency (MNF)	$\frac{\sum_{j=1}^{M}f_jP_j}{\sum_{j=1}^{M}P_j}$
9	Peak frequency (PKF)	$max\left(P_j\right)$
10	Median frequency (MDF)	$\sum_{j=1}^{MDF}P_j = \sum_{j=MDF}^{M}P_j = \frac{1}{2}\sum_{j=1}^{M}P_j$
11	Mean power (MNP)	$\frac{1}{M}\sum_{j=1}^{M}P_j$
12	Total power (TOP)	$\sum_{j=1}^{M}P_j$
13	1st spectral moment (SM_1)	$\sum_{j=1}^{M}f_jP_j$
14	2nd spectral moment (SM_2)	$\sum_{j=1}^{M}f_j^2P_j$

T a b l e 2.

No.	Feature Name	Equation
15	3rd spectral moment (SM_3)	$\sum_{j=1}^{M} f_j^3 P_j$
16	Central frequency variance (VCF)	$\frac{SM_2}{SM_0} - \left(\frac{SM_1}{SM_0}\right)^2$
17–20	Auto-regressive coefficients	$x_i = \sum_{p=1}^{P} AR_p x_{i-p} + w_i$

Knee angle quantization. The human knee joint has a typical range of motion (ROM) from 0° when fully extended to 140° when maximally flexed. In the present study, the ROM ranges from the KA = 0° when in standing position to the KA = 115° when sitting on a chair. The KA is quantized into one of the five classes 0 (KA < 15), 30 (15 < KA ≤ ≤ 45), 60 (45 < KA ≤ 75), 90 (75 < KA ≤ 105), and 120 (105 < KA). The quantized KA is used as a response variable for the classifier.

Classifier. A classifier is a program/algorithm that takes input data instances and predicts the class they belong to. The present study makes use of a support vector machine (SVM) classifier to predict one of the five KS classes. The SVM is a kernel-based approach popular for machine-learning tasks involving regression and classification. It was successfully used in several applications ranging from image processing [27] to speech recognition [28] and text classification [29].

The performance of the SVM classifier depends on a choice of the kernel function. The current study uses the RBF kernel. Two parameters applied, the cost of penalty C and the kernel function parameter γ, must be set appropriately. The value choice for C influences the classification outcome. A large value of C results in a very low misclassification rate in the training phase and a very high misclassification rate during the testing phase, whereas a low value of C results in unsatisfactory results making the model useless [30].

The parameter γ influences the partitioning outcome within the feature space and, thus, exerts a much higher influence on the classifier outcomes than the penalty factor C. An excessively large value for parameter γ results in over-fitting, whereas an unduly small value results in under-fitting [31, 32]. Both parameters, C and γ, can be appropriately selected by employing a grid search [33].

BPSO-based optimal feature selection. In the present study, 20 particles were considered. Each particle is randomly initialized within an n-dimensional space, where n represents the number of EMG features considered. Three initialization strategies have been studied. These are large initialization (LI), which initializes each particle with random combination of the large number of features (80% of total features), small initialization (SI), which initializes each particle with a random combination of the small number of features (20% of the total features), and mixed initialization (MI), which initializes 60% of particles with a random combination of the small number of features and remaining 40% of the particles with a random combination of the large feature number. The present study was aimed at achieving the maximum classification accuracy (minimum classification error) by utilizing a minimum number of the features. The CA is evaluated mathematically as:

$$CA = \frac{TP + TN}{TP + TN + FP + FN}, \tag{7}$$

where TP represents the true positive, FP represents the false positive, TN represents the true negative, and FN represents the false negative. In each iteration, the CA is evaluated for each particle. The CA obtained is compared with the CA of the previous best particle position P_{best}. The position P_{best} is updated to the particle's position in a case the particle CA is better. Similarly, the CA obtained is compared with the CA of the swarm's best position G_{best}, and if the particle CA is better, G_{best} is updated to the present particle position. The

particle velocity and position are updated according to Eq. 1 and Eq. 3 respectively. The inertial weight is varied from w_{max} to w_{min} linearly according to Eq. 8:

$$w = w_{max} - \frac{\left(w_{max} - w_{min}\right) \cdot It}{MaxIT}, \quad (8)$$

where It represents the present iteration, and $MaxIT$ is the maximum iteration allowed in the present study. The process is repeated until the termination conditions are met. Figure 2 shows the flowchart of the PSO-based feature selection and classifier parameter of the optimization system.

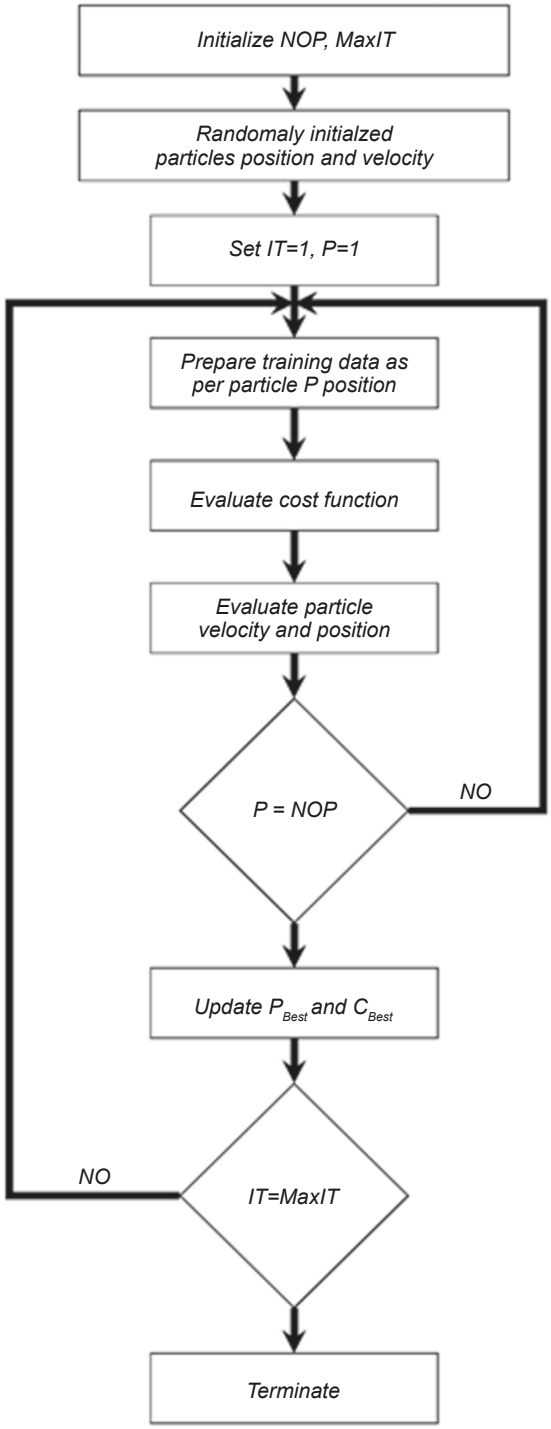

F i g. 2. Flow chart of the binary particle swarm optimization-based feature selection.

Parameters. The number of particles in the swarm was set to 30. The personal learning factor C_1 and the global learning factor C_2 were set to 2. The range of velocity $[-v_{max}, v_{max}]$ was kept at [−5, 5]. The parameters w_{max} and w_{min} were set to 0.9 and 0.4 respectively. Ten-fold cross-validation was performed on the CA obtained for each subject; IBM SPSS Statistics 21 software was used to compare the numerical results.

RESULTS AND DISCUSSION

In our study, the sEMG signals and KA were measured while performing a simple daily-life activity of standing up from and sitting down in a chair. Figure 3 shows the EMG signals recorded from the VL and RF muscles and KA of subject 5 during the present study. For appropriate parameter selection of the RBF kernel, a two-step grid selection was performed, and parameters with the smallest cross-validation error were selected. In the first step, the grid search was performed within a wide range $\left[10^{-3}\ \text{to}10^{3}\right]$ for C and $\left[10^{-3}\,\text{to}10^{3}\right]$ for γ with a logarithmic grid. Tenfold cross-validation was performed, and the classification error was measured. Subsequently, the range in the second step was narrowed down to $\left[10^{-1}\,\text{to}10^{3}\right]$ for C and $\left[10^{0}\,\text{to}10^{3}\right]$ for γ with the logarithmic grid.

Figure 4 shows a heat map of the cross-validated classification error. The average values of the parameters C and γ for all subjects came to 160.32 and 23.00 respectively. Table 3 presents the results of ANOVA on the CA obtained at using the three initialization strategies (LI, SI, and MI) for subject S2. It was found that the results may be considered statistically the same ($P = 0.0675$). However, the MI is preferred for the rest of the study, as it contains a mix of the particles with a large number of features, as well as particles with a small number of features. The performance of the SVM classifier with binary particle swarm optimization-based feature selection (BPSOFS) for predicting the KA was compared with the performance of an SVM classifier fed with all the features. Table 4 presents the result of the tenfold cross-validated CA. A paired *t* test conducted on the CA obtained with and without feature selection demonstrated that the CA obtained with BPSOFS is statistically the same with respect to that obtained by using all 40 features ($P > 0.05$). Table 4 indicates that the feature subset evolved using BPSOFS has, on average, 11.5± ±0.63 features. Thus, BPSOFS obtains statistically the same CA when using only around 30% of the total features.

Table 5 presents the feature subset selected for different subjects and the *P* value obtained for the paired *t* test between the CA obtained with the same SVM classifier using BPSOFS and the CA obtained

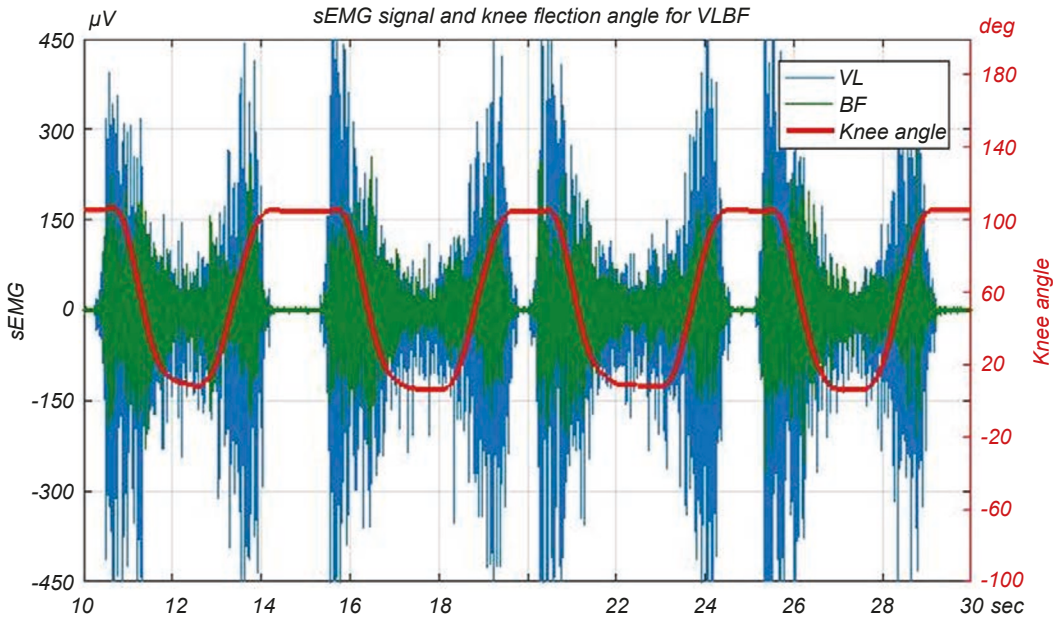

F i g. 3. Knee angles and EMG signals recorded from the VL and BF in the study.

using the same classifier but all the features. The feature subset is a mix of both time domain and frequency domain features. For all subjects, the value of *P* obtained was greater than 0.05, indicating that a difference in the CA with the feature set selected using BPSOFS is statistically insignificant.

The existing literature [12–16, 34] with regard to lower limb movements focuses mainly on predicting the locomotion modes, such as level-ground walking and ascending/descending ramps and stairs. The closest match of the literature data to the results of our study is the continuous estimation of the joint angles from sEMG signals using a back-propagation neural network [18] and that of predicting the KA using a multilayer perceptron neural network [17]. The leg extension exercise in the Zhang et al.

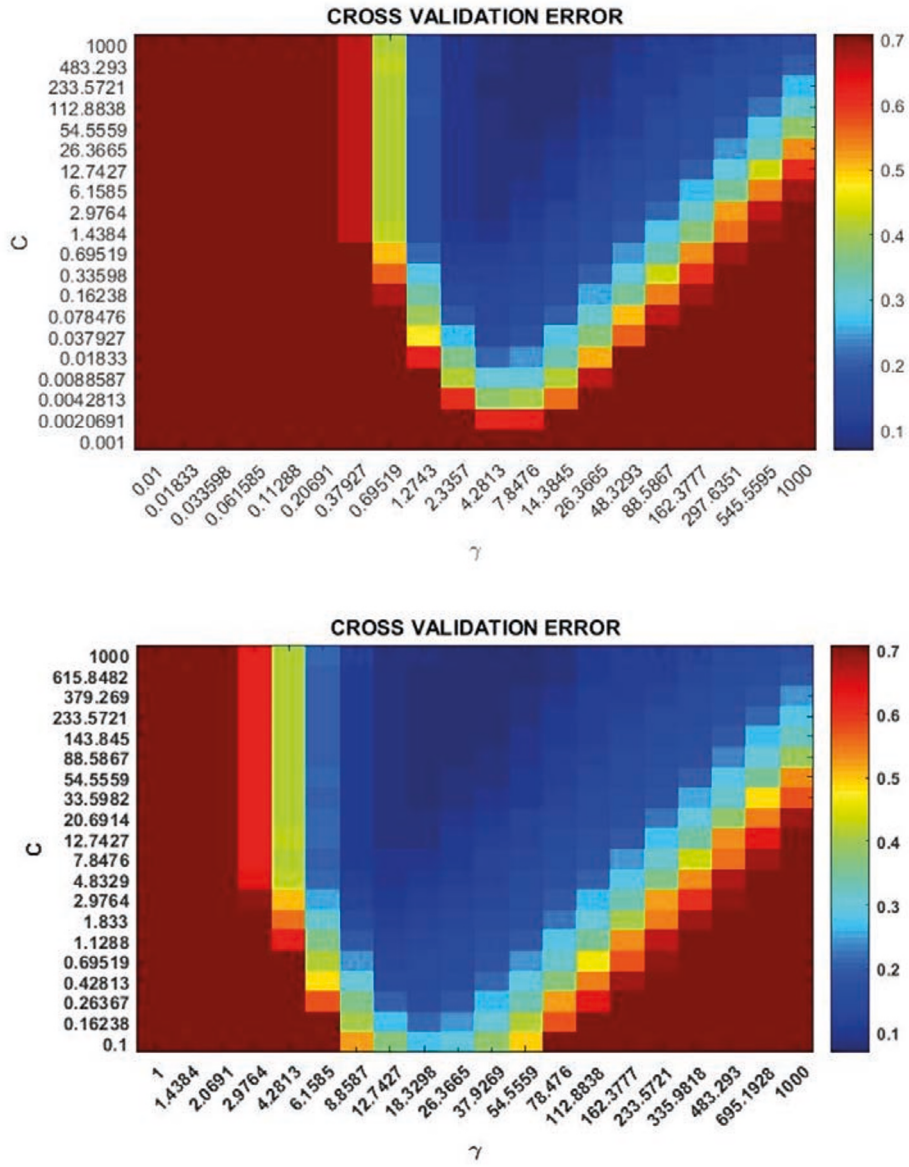

F i g. 4. Heat map showing values of the cross-validation error.

T a b l e 3. Results of the ANOVA Test on CA Obtained Using Different Initialization Techniques

	Sum of the squares	*Df*	Mean square	*F*	*P*
Between groups	0.003	2	0.001	3.430	0.067
Within groups	0.010	27	0.000		
Total	0.012	29			

T a b l e 4. Results Obtained for Classification with and without BPSOFS

Subject	BPSOFS		CA (%) with all features (without BPSO)
	Average number of the features selected	Average CA (%)	
S1	8.9 ± 0.99	92.40	93.99
S2	11.7 ± 1.49	90.32	91.65
S3	11.5 ± 0.97	92.68	93.07
S4	11.9 ± 1.28	86.73	86.92
S5	12.8 ± 0.78	90.92	90.09
S6	13.6 ± 0.84	92.04	92.26
S7	10.8 ± 1.39	92.45	93.57
S8	12 ± 1.15	92.67	93.15
S9	10.5± 1.79	89.67	90.98
S10	11.3 ± 1.82	87.26	89.78
S11	11.4 ± 1.07	91.87	92.40
S12	11.6 ± 0.96	92.06	92.95
Average	11.5 ± 1.63	90.92	91.73

T a b l e 5. Features Selected with BPSOFS and Results of the Paired t-Test

Subject	BPSOFS		*P* in the paired *t*-test
	Number of the features selected	Features selected	
S1	9	F1, F3, F7, F21, F23, F27, F28, F31, F35	0.05
S2	12	F1, F3, F5, F8, F11, F15, F21, F23, F27, F28, F31, F35	0.05
S3	12	F1, F3, F5, F8, F11, F15, F21, F23, F27, F28, F31, F35	0.05
S4	12	F1, F3, F7, F8, F11, F15, F21, F23, F25, F28, F31, F35	0.05
S5	12	F1, F3, F5, F8, F11, F15, F21, F23, F25, F28, F31, F35	0.05
S6	14	F1, F3, F5, F7, F8, F11, F15, F21, F23, F25, F27, F28, F31, F35	0.05
S7	11	F1, F3, F7, F8, F11, F21, F23, F28, F31, F35	0.05
S8	13	F1, F3, F7, F8, F11, F15, F21, F23, F25, F27, F28, F31, F35	0.05
S9	11	F1, F3, F7, F8, F11, F15, F21, F23, F27, F28, F31	0.05
S10	12	F1, F3, F7, F8, F11, F15, F21, F23, F25, F27, F31, F35	0.05
S11	12	F1, F3, F5, F8, F11, F15, F21, F23, F27, F28, F31, F35	0.05
S12	12	F1, F3, F7, F8, F11, F15, F21, F25, F27, F28, F31, F35	0.05

study [18] can be considered a close match to the activity (sit to stand) in the present paper. The approach adopted in our research work is altogether different as the KA range has been divided into five levels/classes, and the KA class is predicted from features of the sEMG signals. The average classification error measured in the present study is 9.1%, compared with the average RMS error in KA prediction reported by Zhang et al. [18] for leg extension using a small load (12.7°).

Thus, the performance of a BPSOFS in predicting the class of the KA from sEMG signals recorded from the involved muscles (VL and BF) of the lower limb has been studied. The KA was quantized into five levels/classes. Twenty features per muscle were extracted from the segmented sEMG signal and fed to the SVM classifier. A BPSO technique was used to select the feature subsets. The results obtained indicate that the SVM classifier with BPSOFS technique, when using about 30% of the total features, achieved the average classification accuracy of 90.02%, which is statistically similar to that obtained with the SVM classifier using all the features ($P > 0.05$). The proposed scheme can be used to develop a lower limb exoskeleton.

The research protocol for the current study is in accordance with the Helsinki Declaration and was approved by the Institute's research board. All subjects involved gave their preliminary written concent.

The authors, I. S. Dhindsa, R. Gupta, and R. Agarwal, declare that the research was conducted in the absence of any conflicts with respect to commercial or financial relationships and those between the co-authors.

REFERENCES

1. I. Guyon and A. Elisseeff, "An introduction to variable and feature selection," *J. Mach. Learn. Res.*, **3**, 1157–1182 (2003), doi:10.1162/153244303322753616.
2. H. Banka and S. Dara, "A Hamming distance based binary particle swarm optimization (HDBPSO) algorithm for high dimensional feature selection, classification and validation," *Pattern Recognit. Lett.*, **52**, 94–100 (2015).
3. R. Eberhart and J. Kennedy, "A new optimizer using particle swarm theory," In: *MHS'95. Proc. Sixth Int. Symp. Micro Machine Human Sci.*, *IEEE*, 39–43 (1995).
4. R. Boostani and M. H. Moradi, "Evaluation of the forearm EMG signal features for the control of a prosthetic hand," *Physiol. Meas.*, **24**, No. 2, 309–319 (2003), doi: 10.1088/0967-3334/24/2/307.
5. L. Hargrove, K. Englehart, and B. Hudgins, "A training strategy to reduce classification degradation due to electrode displacements in pattern recognition based myoelectric control," *Biomed. Signal Process. Control*, **3**, No. 2, 175–180 (2008).
6. H.-P. Huang, Y.-H. Liu, L.-W. Liu, and C.-S. Wong, "EMG classification for prehensile postures using cascaded architecture of neural networks with self-organizing maps," *Proc. IEEE Int. Robot. Autom.*, **1**, 1497–1502 (2003), doi:10.1109/ROBOT.2003.1241803.
7. M. Zardoshti-Kermani, B. C. Wheeler, K. Badie, and R. M. Hashemi, "EMG feature evaluation for movement control of upper extremity prostheses," *IEEE Trans. Rehabil. Eng.*, **3**, No. 4, 324–333 (1995).
8. A. Phinyomark, F. Quaine, S. Charbonnier, et al., "EMG feature evaluation for improving myoelectric pattern recognition robustness," *Expert Syst. Appl.*, **40**, No. 12, 4832–4840 (2013), doi:10.1016/j.eswa.2013.02.023.
9. K. Englehart, B. Hudgins, P. A. Parker, and M. Stevenson, "Classification of the myoelectric signal using time-frequency based representations," *Med. Eng. Phys.*, **21**, No. 6–7, 431–438 (1999), doi: 10.1016/s1350-4533(99)00066-1.
10. J.-U. Chu, I. Moon, and M.-S. Mun, "A real-time EMG pattern recognition system based on linear-nonlinear feature projection for a multifunction myoelectric hand," *IEEE Trans. Biomed. Eng.*, **53**, No. 11, 2232–2239 (2006).
11. K. E. Member, B. H. Member, P. A. Parker, and S. Member, "A wavelet based continuous classification scheme for multifunction myoelectric control," *IEEE Trans. Biomed. Eng.*, **48**, No. 3, 1–31 (2001).
12. H. Huang, F. Zhang, L. J. Hargrove, et al., "Continuous locomotion-mode identification for prosthetic legs based on neuromuscular--mechanical fusion," *IEEE Trans. Biomed. Eng.*, **58**, No. 10, 2867–2875 (2011), doi: 10.1109/TBME.2011.2161671.
13. R. Gupta and R. Agarwal, "Electromyographic signal-driven continuous locomotion mode identification module design for lower limb prosthesis control," *Arab. J. Sci. Eng.* (2018), doi:10.1007/s13369-018-3193-3.
14. R. Gupta, I. S. Dhindsa, and R. Agarwal, "Continuous angular position estimation of human ankle during unconstrained locomotion," *Biomed. Signal Process. Control*, **60**, 101968 (2020).
15. R. Gupta and R. Agarwal, "Continuous human locomotion identification for lower limb prosthesis control," *CSI Trans. ICT*, **6**, 1–15 (2017), doi:10.1007/s40012-017-0178-4.
16. H. Huang, T. A. Kuiken, and R. D. Lipschutz, "A strategy for identifying locomotion modes using surface electromyography," *IEEE Trans. Biomed. Eng.*, **56**, No. 1, 65–73 (2009), doi: 10.1109/TBME.2008.2003293.
17. A. L. Delis, J. L. A. Carvalho, A. F. Da Rocha, et al., "Estimation of the knee joint angle from surface electromyographic signals for active control of leg prostheses," *Physiol. Meas.*, **30**, No. 9, 931–946 (2009), doi: 10.1088/0967-3334/30/9/005.
18. F. Zhang, P. Li, Z.-G. Hou, et al., "sEMG-based continuous estimation of joint angles of human legs by using BP neural network," *Neurocomputing*, **78**, No. 1, 139–148 (2012).
19. I. S. Dhindsa, R. Agarwal, and H. S. Ryait, "Performance evaluation of various classifiers for predicting knee angle from electromyography signals," *Expert Syst.*, **36**, No. 3, e12381 (2019), doi:10.1111/exsy.12381.
20. C.-L. Huang and J.-F. Dun, "A distributed PSO–SVM hybrid system with feature selection and parameter optimization," *Appl. Soft Comput.*, **8**, No. 4, 1381–1391 (2008).
21. Eberhart and Y. Shi, "Particle swarm optimization: developments, applications and resources," *Proc. 2001 Congr. Evol. Comput.*, **1**, 81–86 (2001), doi: 10.1109/CEC.2001.934374.
22. J. Kennedy and R. C. Eberhart, "A discrete binary version of the particle swarm algorithm," *1997 IEEE Int. Conf. Sys., Man Cybern. Comput. Cybern. Simul.,* **5**, 4104–4108 (1997), doi: 10.1109/ICSMC.1997.637339.
23. I. S. Dhindsa, R. Agarwal, and H. S. Ryait, "Principal component analysis-based muscle identification for myoelectric-controlled exoskeleton knee," *J. Appl. Stat.*, **44**, No. 10, 1707–1720 (2017), doi:10.1080/02664763.2016.1221907.
24. B. Frericks, "The recommendations for sensors and sensor placement procedures for surface electromyography," *SENIAM Deliv. 8, Eur. Recomm. Surf. Electromyogr.*, 15–53 (1999).
25. L. J. Hargrove, G. Li, K. B. Englehart, and B. S. Hudgins, "Principal components analysis preprocessing for improved classification accuracies in pattern-recognition-based myoelectric control," *IEEE Trans. Biomed. Eng.*, **56**, No. 5, 1407–1414 (2009), doi: 10.1109/TBME.2008.2008171.
26. B. Hudgins, P. Parker, R. N. Scott, B. Hudgins, P. Parker, and R. Scott, "A new strategy for multifunction myoelectric control," *IEEE Trans. Biomed. Eng.*, **40**, No. 1, 82–94 (1993), doi: 10.1109/10.204774.
27. J. Virmani, V. Kumar, N. Kalra, and N. Khandelwal, "SVM-based characterization of liver ultrasound images using wavelet packet texture descriptors," *J. Digit. Imaging*, **26**, No. 3, 530–543 (2013), doi: 10.1007/s10278-012-9537-8.

28. A. Ganapathiraju, J. E. Hamaker, and J. Picone, "Application of support vector machines to speech recognition," *IEEE Trans. Signal Process.*, **52**, No. 8, 2348–2355 (2004), doi:10.1109/TSP.2004.831018.
29. S. Tong and D. Koller, "Support vector machine active learning with applications to text classification," *J. Mach. Learn. Res.*, **2**, No. Nov, 45–66 (2001), doi:10.1162/153244302760185243.
30. S.-W. Lin, K.-C. Ying, S.-C. Chen, and Z.-J. Lee, "Particle swarm optimization for parameter determination and feature selection of support vector machines," *Expert Syst. Appl.*, **35**, No. 4, 1817–1824 (2008), doi:10.1016/j.eswa.2007.08.088.
31. M. Pardo and G. Sberveglieri, "Classification of electronic nose data with support vector machines," *Sensors Actuators B Chem.*, **107**, No. 2, 730–737 (2005).
32. S.-C. Chen, S.-W. Lin, and S.-Y. Chou, "Enhancing the classification accuracy by scatter-search-based ensemble approach," *Appl. Soft Comput.*, **11**, No. 1, 1021–1028 (2011).
33. C.-W. Hsu, C.-C. Chang, and C.-J. Lin, "A practical guide to support vector classification" (2003).
34. R. Gupta and R. Agarwal, "sEMG interface design for locomotion identification," *Int. J. Electr. Comput. Eng.*, **11**, No. 2, 66–75 (2017).